OPEN ACCESS

Impact of drusen and drusenoid retinal pigment epithelium elevation size and structure on the integrity of the retinal pigment epithelium layer

Ferdinand Schlanitz,[1] Bernhard Baumann,[2] Stefan Sacu,[1] Lukas Baumann,[3] Michael Pircher,[2] Christoph K Hitzenberger,[2] Ursula Margarethe Schmidt-Erfurth[1]

[1]Department of Ophthalmology and Optometry, Medical University of Vienna, Vienna, Austria
[2]Center for Medical Physics and Biomedical Engineering, Medical University of Vienna, Vienna, Austria
[3]Section for Medical Statistics, Center for Medical Statistics, Informatics and Intelligent Systems, Medical University of Vienna, Vienna, Austria

Correspondence to
Professor Ursula Margarethe Schmidt-Erfurth, Department of Ophthalmology and Optometry, Medical University of Vienna, Währinger Gürtel 18-20, 1090 Vienna, Austria; ursula.schmidt-erfurth@meduniwien.ac.at

Received 11 January 2018
Accepted 5 April 2018
Published Online First 29 April 2018

To cite: Schlanitz F, Baumann B, Sacu S, *et al*. *Br J Ophthalmol* 2019;**103**:227–232.

ABSTRACT

Purpose To evaluate the impact of drusen size and structure on retinal pigment epithelium (RPE) and photoreceptor layers in eyes with early to intermediate age-related macular degeneration (AMD) using polarisation-sensitive optical coherence tomography (OCT).

Design Retrospective investigation of an observational cross-sectional study.

Participants Patients with early to intermediate AMD.

Methods Twenty-five eyes of 25 patients with drusen were imaged with polarisation-sensitive OCT using macular volume scans. Each scan was manually graded for six distinct drusen characteristics and the integrity of both the overlying RPE and photoreceptor layer. The central scan of each single druse, as well as its diameter and location, were selected for statistical calculations.

Results A total number of 5933 individual drusen including their adjacent RPE and photoreceptor layer were evaluated. 41.3% of all drusen demonstrated an intact overlying RPE; in 28.1% the RPE layer was irregular, but continuous. In 30.6%, the RPE layer signal was discontinuous above the area of drusen. The level of RPE alteration was significantly related to shape ($p<0.001$), internal reflectivity ($p<0.001$) and homogeneity ($p<0.001$) of the drusen and their diameter, with a higher probability for larger drusen to have a discontinuous RPE (OR 3.2, $p<0.001$). The number of drusen showing overlying foci or an altered photoreceptor layer was too small to be conclusive, but showed a trend towards an altered RPE if present.

Conclusions Polarisation-sensitive OCT reveals a correlation between specific drusen characteristics and the integrity of the overlying RPE layer. Drusen diameter and configuration were significantly associated with RPE loss.

INTRODUCTION

Drusen represent a clinical hallmark of age-related macular degeneration (AMD).[1] Recent surveys from the Blue Mountains Eye Study underline the importance of drusen for progression risk.[2] These observations were based on fundus photography and did not consider the morphological variability drusen can show in histological as well as in optical coherence tomography (OCT).[3–7] Furthermore, longitudinal OCT studies brought new insight into drusen development; however, risk calculation for the individual patient still remains an open question for clinicians.[8–10]

Degenerative changes in the retinal pigment epithelium (RPE) layer are considered as an important sign of disease progression, a process that is eventually accompanied by loss of adherent photoreceptors.[6 11–13] Several studies assume a strong correlation between drusen formation and pathological processes within the RPE cell as a fulcrum in AMD pathogenesis.

The purpose of this study was to investigate the relationship between distinct drusen characteristics seen by OCT imaging and their impact on the overlying RPE and retinal integrity. For this purpose, polarisation-sensitive OCT imaging was used, which combines the high-resolution images of the spectral domain OCT with a specific detection of melanin.[14–17] Pilot studies were able to demonstrate the potential of polarisation-sensitive OCT to image the RPE in patients with AMD and drusen,[18 19] and in a previous investigation characteristic polarisation-sensitive features of drusen were described.[5]

In the present study, the data from the cohort of this investigation[5] were re-evaluated in order to determine correlations between drusen characteristics, including their extensiveness, and the integrity of RPE and photoreceptor layer adherent to the underlying drusen.

METHODS

The cohort presented in this observational cross-sectional study is the same investigated in a prior study published in 2015.[5]

Inclusion/exclusion criteria

Patients were selected according to the standard classification introduced by the Age-Related Eye Disease Study (AREDS).[20] Only eyes with drusen of AREDS categories 2 and 3 were included. Category 2 encompasses the presence of extensive small (<63 µm in diameter) to non-extensive intermediate drusen (between 63 and 125 µm) or pigment epithelial abnormalities in at least one eye. Category 3 is defined by extensive intermediate to large (>125 µm) drusen and/or non-central geographic atrophy in at least one eye.[20] However, patients presenting with signs of geographic atrophy were excluded, as well as patients with other eye diseases than AMD and with previous surgery other than uncomplicated cataract surgery.

Imaging procedures

Patients meeting the protocol criteria were informed about the study aims and procedures. After given informed consent, patients underwent a standardised examination. Best-corrected visual acuity (BCVA) was obtained and mydriatic eye-drops were administered. Digital photographs of the fundus were taken (FF 450plus, Carl Zeiss Meditec, Dublin, California). Using the Spectralis spectral domain OCT system (Heidelberg Engineering, Germany), the following images of the retina were obtained, with the automated real-time tracking mode set at 15 frames: infrared reflectance image, fundus autofluorescence images at 488 nm excitation wavelength and near-infrared fundus autofluorescence images at 787 nm excitation wavelength. Subsequently, retinas were scanned with polarisation-sensitive OCT using a prototype engineered by the Centre for Medical Physics and Biomedical Engineering.[21] As in spectral domain OCT imaging, this system measures the intensity of the backscattered light. Additionally, the device obtains three parameters simultaneously: retardation, fast axis orientation and degree of polarisation uniformity (DOPU).[16] Studies showed that the polarisation state of the backscattered light beam is scrambled by the melanosomes of the RPE cell bodies, thus producing a characteristic DOPU signal which enables the segmentation of the layer of RPE cell bodies.[22] Three-dimensional data sets with 64×1024 volume scan pattern were recorded (20 000 A-scans/s, scan field 20°×20°, approximately 6×6 mm^2). Scans of insufficient quality were repeated until satisfactory results were obtained.

Classification of drusen

Two reviewers independently graded all OCT B-scans of each eye. For this purpose, a custom-made Matlab program was installed that allowed manual segmentation of drusen in the individual B-scans. Drusen were distinguished between small (<63 µm in diameter), intermediate (between 63 and 125 µm) and large drusen (between 125 and 350 µm). RPE elevations larger than 350 µm were classified as drusenoid pigment epithelial detachments (DPED).[23] Drusen below a diameter of 25 µm were excluded from further statistical analysis as their characterisation is limited by the imaging resolution.

Subsequently, drusen were classified using the classification system presented by Khanifar *et al*.[3] This classification differentiates between the shape of the RPE elevation (convex, concave or saw-toothed), the reflectivity (low, medium or high) and the homogeneity (homogeneous reflectivity, non-homogeneous with or without a central core) of the drusen content and the presence or absence of hyper-reflective foci above (see figure 1).

For classification of the polarisation-sensitive information, this classification system was expanded by two further parameters introduced in our previous work[5]: depolarising structures within the druse (single depolarising core, non-homogeneous depolarising structures, complete fill-out of the druse with depolarising material), and the presence or absence of depolarising foci above the druse (also see figure 1).

Evaluation of RPE and photoreceptor layer

The integrity of the RPE layer was assessed based on the depolarising signal (see figure 1, bottom left panel): The consistency of this signal was scored as (1) normal (continuous depolarising RPE band, without difference in appearance compared with drusen-free areas of the same B-scan), (2) continuous, but irregular, (3) presence of a single focal signal disruption, (4) discontinuity not exceeding one-third of the RPE layer, (5) discontinuity not exceeding two-thirds of the RPE layer, (6) discontinuity exceeding two-thirds of the RPE contour, and (7) complete absence of signal continuity with or without dot-like signal spots. For assessment of concomitant alterations, the continuity of the inner/outer segment band (IS/OS) was examined. OCT features overlying areas with drusen were compared and screened for

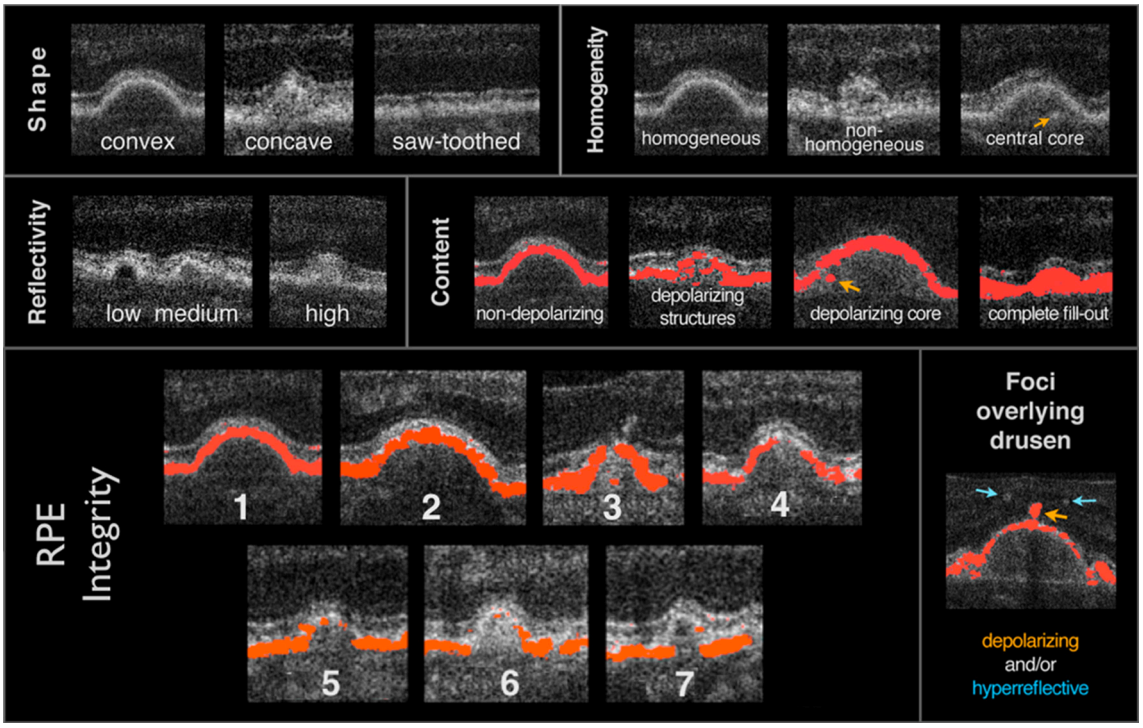

Figure 1 Classification of drusen. Drusen were classified according to their shape, homogeneity and internal reflectivity, as well as depolarising contents (top two rows). Furthermore, the consistency of the retinal pigment epithelium (RPE) signal—depicted in red colour—was evaluated, ranging from normal (1) to a complete absence of depolarising material (7). The presence of overlying foci—depolarising or not—was also assessed.

allocated discontinuities of the IS/OS. In case of foci in the inner retinal layers, a possible shadow was accounted for any inconsistencies in the layers below and noted separately. RPE or IS/OS discontinuities or irregularities were only noted when they extended horizontally beyond the shadow.

Data analysis and statistical methods

Location, height and all other predefined parameters of individual drusen were displayed in a drusen map for each eye. Within this map, single drusen were identified by their definition as round focal accumulations. The slice of each delineated druse that was closest to the assumed drusen centre (ie, with the largest drusen diameter) was selected and the determined parameters were transferred into SPSS for further statistical analysis.

To assess the agreement rate between the two graders, Cohen's kappa statistics were performed. In order to find features of drusen that influence the overlying RPE integrity, a binary categorisation of the RPE integrity was used, with 'normal' and 'irregular' in one group and all other discontinuous categories in the other group. The considered explanatory variables were drusen diameter (continuous, logarithmised because of right-skewed distribution), shape, reflectivity, drusen content and homogeneity (all categorical). Univariate logistic mixed models were performed, with the binary RPE integrity as the dependent variable and the respective drusen feature as the independent variable. Additionally the eye was specified as a random effect.

For the categorical explanatory variables, an analysis of variance was computed at first, followed by pairwise post-hoc comparisons using the Tukey correction. Furthermore a multivariate model was calculated, using all the explanatory variables.

The significance level was set to 0.05 for all tests.

Statistical analyses were carried out using PASW Statistics V.18.0, R Project and Matlab. The library lme4 was used to compute the mixed models, while the library multcomp was used for the post-hoc comparisons.

RESULTS

Twenty-five eyes of 25 patients were examined. Fourteen patients were female, and the mean age was 72 years (SD 6.0, range 60–85). The mean BCVA was 0.9 (range 0.6–1.25), and five patients were pseudophakic. A total number of 5933 drusen were analysed, with a mean diameter of 114 µm (SD 69.5, range 29–346). The mean number of drusen counted in the drusen maps was 246 (SD 142, range 26–648). Furthermore, a total number of 291 DPEDs were detected, with a mean diameter of 504 µm (SD 163, range 352–1371).

Interobserver agreement for grading the RPE was good with a weighted $\kappa=0.62$ (Cohen's kappa coefficient). In 41.3% of all drusen and 16.3% of DPED, there was an intact overlying RPE. In 28.1% of drusen and 26.3% of DPED, the RPE layer signal was irregular, but continuous (grade 2). In 30.6% of drusen and 57.4% of DPED, there was a discontinuous overlying RPE signal, ranging from a single distinct lesion (grade 3, 22.8% drusen and 42.2% DPED) to complete absence (grade 7, 0.7% drusen, no DPED).

The mean drusen diameter presenting a morphologically intact RPE layer was 97 µm, and for lesions with an irregular RPE band 134 µm. With progressive RPE alteration, the mean diameter of the drusen consistently increased, reaching its apex at grade 4 with up to one-third of the overlying RPE signal missing and a mean diameter of 196 µm. Beyond that threshold, the mean drusen diameter decreased, with a mean of 94 µm for grade 7 lesions and almost no remaining depolarising signal in the overlying RPE (see figure 2). The size of the drusen had a significant influence on the dichotomised RPE integrity, with a higher probability for larger drusen to have a discontinuous overlying RPE layer (OR 3.185, $p<0.001$).

The integrity of the dichotomised RPE signal further correlated to the shape of the druse. Concave-shaped drusen were significantly more often accompanied by a discontinuous RPE signal than convex-shaped drusen (OR 0.631, $p<0.001$), and 42.1% of all convex-shaped drusen exhibited a normal overlying RPE layer, vs 24.5% of the concave-shaped drusen. Only 7.9% of drusen with a saw-tooth appearance had a normal overlying RPE, while 60.5% an irregular thickness.

A low as well as a medium internal reflectivity was significantly associated with a discontinuous RPE layer compared with drusen with high reflectivity (OR 0.355, respectively, 0.528,

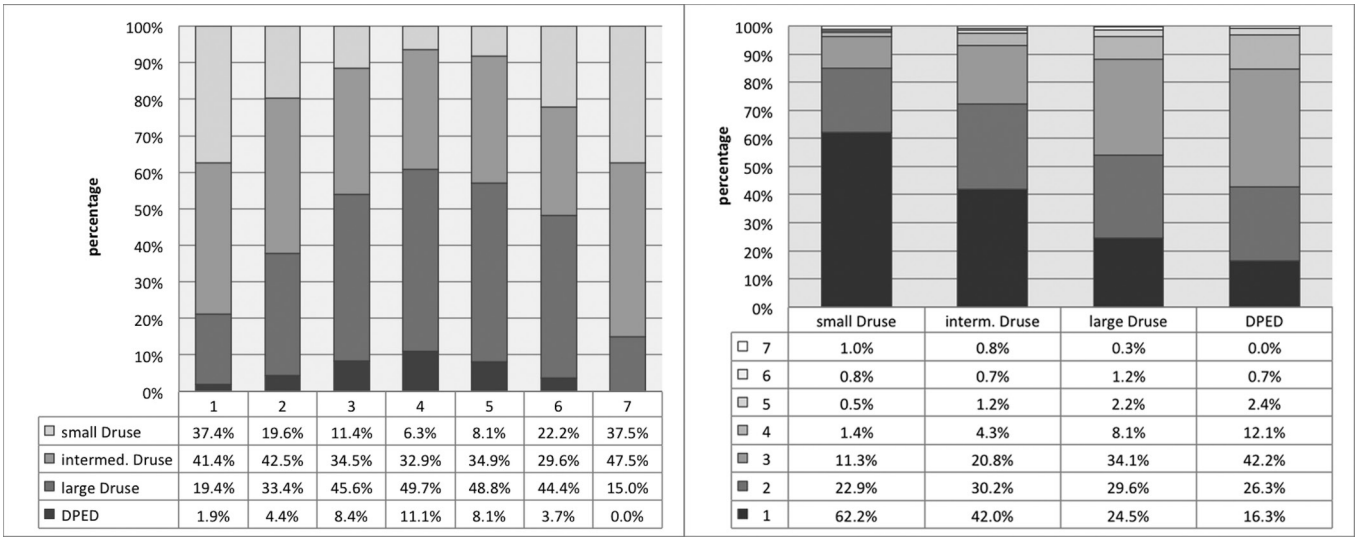

Figure 2 Relationship between drusen size and integrity of the RPE layer. On the left image, the RPE integrity ranging from 1 (normal) to 7 (absence) forms the x-axis, and drusen size is indicated by colours; thus the shift of size throughout the RPE layer integrity states can be seen. On the right image, the x-axis indicates drusen size, and the colours display integrity levels. DPED, drusenoid pigment epithelial detachment; RPE, retinal pigment epithelium.

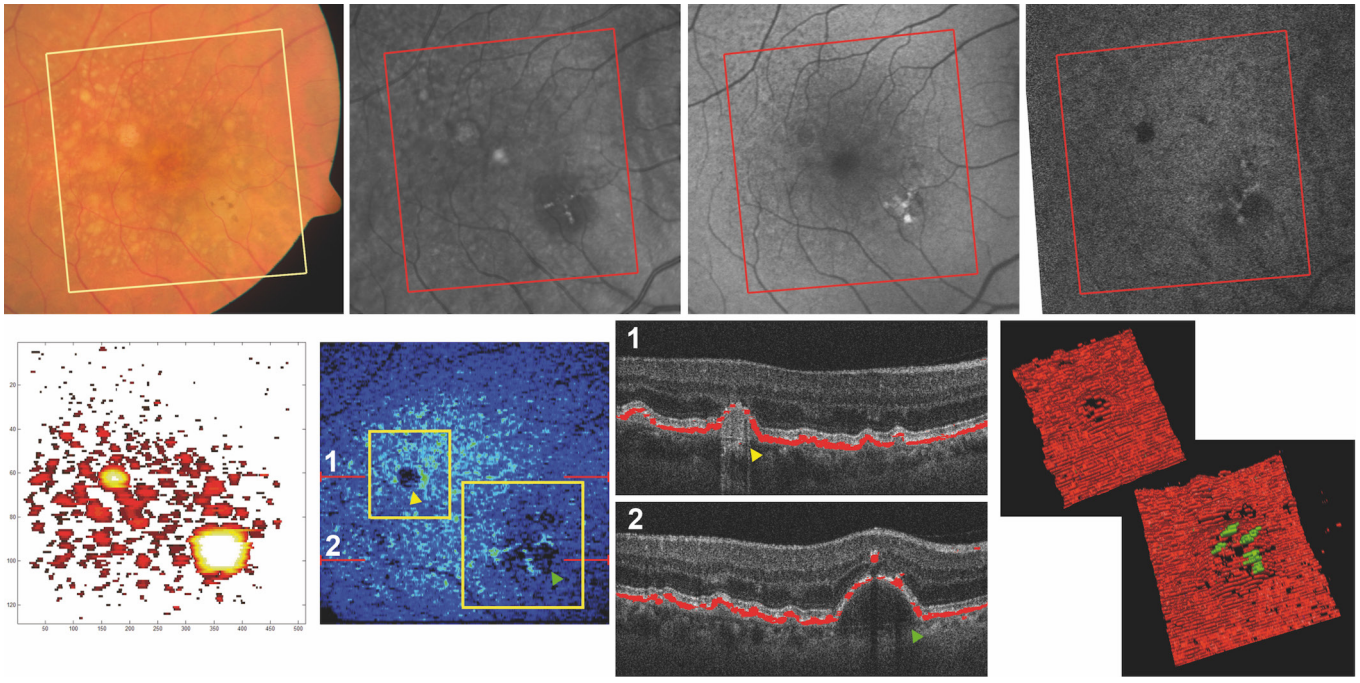

Figure 3 Multimodal imaging and 3D reconstruction in detail. Top row, from left to right: fundus photography of the foveal area of a 67-year-old patient, followed by the infrared reflectance, the fundus autofluorescence and the near-infrared fundus autofluorescence images. The bottom row shows the manually segmented drusen map on the left, followed by the automatically generated thickness map of the RPE signal. The red lines indicate the position of the B-scans aside, and the yellow frames the positions of the 3D reconstructions on the far right. In (1) a druse with a grade 5 loss of RPE signal is shown (yellow arrowhead), while (2) shows a large DPED with pigment migration (green arrowhead). In the bottom right images, these drusen are shown in 3D, with pigment migration signal coloured in green. 3D, three-dimensional; DPED, drusenoid pigment epithelial detachment; RPE, retinal pigment epithelium.

p<0.001). Similar correlations were found between the homogeneity of the internal reflectivity and the RPE condition, with a non-homogeneous internal reflectivity, with or without central core, significantly related to a disintegrated RPE compared with drusen with homogeneous non-depolarising reflectivity (OR 1.652, respectively, 1.379, p<0.001). However, there is no significant difference between both non-homogeneous categories and the RPE integrity, whether they have a core or not (OR 0.835, p=0.394). Drusen with complete fill-out with depolarising material had significantly more often a physiological to

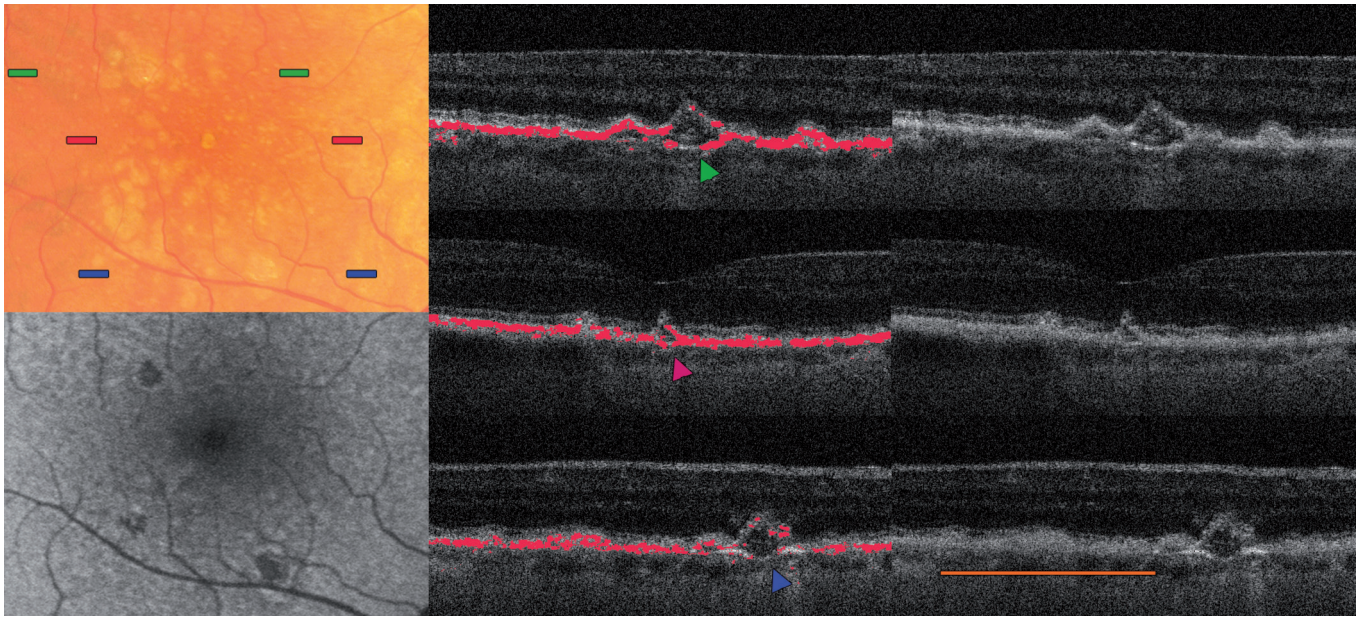

Figure 4 Eye of a 70-year-old woman showing concave drusen (arrowheads). The colour bars on the fundus photography (top left image) indicate the position of the respective B-scans. In the fundus autofluorescence (below), the retinal pigment epithelium (RPE) hypoautofluorescence can be seen. The orange bar in the bottom right image shows a cluster of indifferent drusenoid lesions with irregular RPE coverage, reminding the saw-toothed pattern.

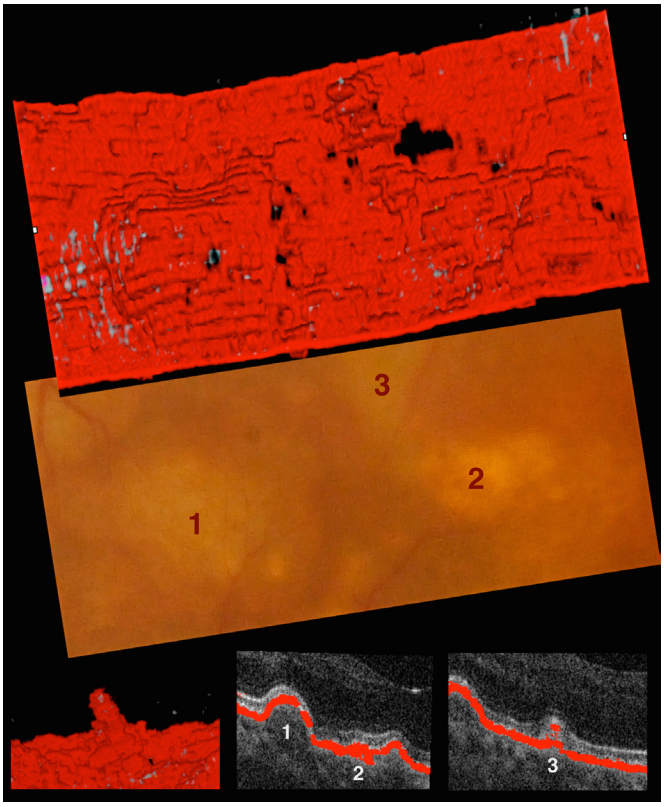

Figure 5 A close-up of three different stages of retinal pigment epithelium (RPE) integrity overlying drusen. The top image shows a three-dimensional (3D) representation of the segmented RPE layer, the corresponding colour fundus photography in the centre and two B-scans of the corresponding region below (width of the B-scans and images above ~1 mm). (1) indicates a large soft druse showing focal lesions within the depolarisation signal, (2) a calcified druse with a fill-out with depolarising material and an irregular RPE shape, and (3) a concave-shaped druse with adjacent RPE lesion, which has an interesting form shown in 3D from another perspective in the bottom left image.

irregular, but continuous adherent RPE layer compared with all other categories (OR compared with non-homogeneous with core: 0.040; without core: 0.048; compared with homogeneous content: 0.067; $p<0.001$), although the grading of the RPE in such drusen is limited.

The significant correlations between RPE integrity and the different drusen features described above were tested in the univariate logistic mixed model.

The number of drusen with a discontinuous IS/OS (1.2% of all drusen) and with foci in the retinal layers (0.3% of all drusen) was too small for statistic calculations. However there was a trend with the IS/OS being disrupted more often in larger drusen and a more frequent presence of overlying foci with lower levels of RPE integrity.

DISCUSSION

In this work, the relationship between drusen parameters on the integrity of the overlying RPE was evaluated. To visualise the RPE layer integrity, polarisation-sensitive OCT was used due to its ability to provide selective identification of melanosomes inside the RPE. As the RPE plays an important role in the pathophysiology of AMD, knowledge of the influence of drusen on RPE integrity potentially allows to differentiate between relevant drusen types for progression of AMD disease. Furthermore, the impact of drusen on the photoreceptor layer was investigated; however, the results were inconclusive.

A significant correlation between drusen size and the overlying RPE condition was demonstrated. Figure 2 shows the relationship between drusen size and progressive RPE disintegrity, representing a bell-shaped figure that might reflect the natural history of drusen in AMD. As drusen grow steadily over time,[9 10] the RPE is increasingly compromised. Balaratnasingam *et al*[9] showed the continuous growth of DPEDs, and furthermore RPE disruptions, the occurrence of which coincided at the later life cycle of DPEDs, shortly before their collapse. Therefore it seems plausible that beyond a threshold level of expansion, the overlying RPE might be destroyed to a level that subsequently leads to a collapse and consequential to a regression of the size of the underlying drusen. Hypothetically, the RPE elevation decreases, but the RPE layer remains irregular, thus possibly developing a facilitating area for advanced stages of AMD. Lesions in the RPE layer could be found at the top of the drusen (see figure 3, B-scan no 1) as well as on their flank (see figures 4 and 5).

However, as a limitation of this study, one has to be careful when interpreting small skip lesions in cases where the RPE is cut diagonally, such as at the base of a large druse, as it might be caused by a calculation error of the DOPU.

Veerappan and colleagues[8] showed in a longitudinal survey that specific morphological characteristics of drusen are predictive of accelerated progression towards atrophic AMD. In the present paper, a correlation between the RPE condition and shape, internal reflectivity and homogeneity of drusen was found, including clinically unapparent lesion types such as a saw-toothed drusen pattern. This drusen type might be the remainder of a collapsed druse (figure 4, yellow bar). Saw-toothed drusen might also originate from cuticular drusen, which tend to protrude into the RPE layer, causing an irregular contour of the layer[4] (also see figure 1 of Schlanitz *et al*[5]). The finding of concave-shaped drusen is unclear, as this shape has not yet been defined by histological studies. Veerappan *et al*[8] found drusen with conical shape were associated with the highest rate of atrophic signs at a 2-year follow-up. The conical/concave shape seems to be a result of the highly distorted RPE coverage, which subsequently either leads to partial resorption of the druse, initiates RPE cell migration towards the inner retinal layers and/or forms a vitelliform lesion.[13 24]

The internal reflectivity as well as drusen homogeneity might represent different biological conditions inside drusen. The finding that drusen with a non-homogeneous internal reflectivity are more often associated with an affected RPE layer might reflect decomposition processes, or the internalisation of residual particles originating from degenerated RPE cells, as shown by various histological investigations; furthermore, cells have been reported in a small number of drusen.[7]

The presence of pigmentary alterations is suspected to be associated with a worse prognosis for AMD progression.[12] However, the number of drusen demonstrating overlying foci was too small to draw general conclusions. An altered IS/OS was also found rarely, despite numerous drusen with discontinuous RPE; this might be caused by the limited capability of OCT imaging to depict subtle alterations of photoreceptors.

In summary, suspected drusen-related risk factors for AMD progression, such as large size and inhomogeneity of its content, were visualised and correlated with different levels of overlying RPE degeneration. The precise observation of the morphological features might help in understanding the pathomechanisms of AMD disease. Monitoring focal changes longitudinally will

highlight the sequence of events to identify the mechanisms of resolution of drusen material and loss of RPE cells.

Correction notice This paper has been corrected since it was published Online First. The first author's first name and surname were transposed and this has since been corrected.

Contributors SF: design of the work, data collection, data analysis, drafting the article. BB: data analysis, critical revision of the article. SS: data analysis and interpretation, critical revision of the article. BL: data analysis and interpretation. PM: data analysis and interpretation. HC: conception of the work, data analysis and interpretation, critical revision of the article. S-EU: design of the work, data interpretation, critical revision and final approval of the article to be published.

Funding CKH has received support by an independent scientific grant (FWF grant P19624-B02, Austrian Science Fund, Vienna, Austria), the European Union (FP7 HEALTH programme grant 201880, FUN-OCT, Brussels, Belgium) and Canon (Tokyo, Japan). S-EU has received support from an independent scientific grant (Herzfelder'sche Familienstiftung, grant AP0044120FF). None of the grantors had any influence on reporting the study data and interpretation of the data. All other authors did not receive any government or non-governmental fundings.

Competing interests None declared.

Patient consent Not required.

Ethics approval The study protocol was approved by the local ethics committee of the Medical University of Vienna and adhered to the Declaration of Helsinki (approval number EK599/2009).

Provenance and peer review Not commissioned; externally peer reviewed.

REFERENCES

1 Jager RD, Mieler WF, Miller JW. Age-related macular degeneration. *N Engl J Med* 2008;358:2606–17.
2 Joachim N, Mitchell P, Burlutsky G, *et al*. The incidence and progression of age-related macular degeneration over 15 Years: the blue mountains eye study. *Ophthalmology* 2015;122:2482–9.
3 Khanifar AA, Koreishi AF, Izatt JA, *et al*. Drusen ultrastructure imaging with spectral domain optical coherence tomography in age-related macular degeneration. *Ophthalmology* 2008;115:1883–90.
4 Spaide RF, Curcio CA. Drusen characterization with multimodal imaging. *Retina* 2010;30:1441–54.
5 Schlanitz FG, Sacu S, Baumann B, *et al*. Identification of Drusen Characteristics in Age-Related Macular Degeneration by Polarization-Sensitive Optical Coherence Tomography. *Am J Ophthalmol* 2015;160:335–44.
6 Hageman GS, Luthert PJ, Victor Chong NH, *et al*. An integrated hypothesis that considers drusen as biomarkers of immune-mediated processes at the RPE-Bruch's membrane interface in aging and age-related macular degeneration. *Prog Retin Eye Res* 2001;20:705–32.
7 Rudolf M, Clark ME, Chimento MF, *et al*. Prevalence and morphology of druse types in the macula and periphery of eyes with age-related maculopathy. *Invest Ophthalmol Vis Sci* 2008;49:1200–9.
8 Veerappan M, El-Hage-Sleiman AM, Tai V, *et al*. Optical coherence tomography reflective drusen substructures predict progression to geographic atrophy in age-related macular degeneration. *Ophthalmology* 2016;123:2554–70.
9 Balaratnasingam C, Yannuzzi LA, Curcio CA, *et al*. Associations between retinal pigment epithelium and drusen volume changes during the lifecycle of large drusenoid pigment epithelial detachments. *Invest Ophthalmol Vis Sci* 2016;57:5479–89.
10 Schlanitz FG, Baumann B, Kundi M, *et al*. Drusen volume development over time and its relevance to the course of age-related macular degeneration. *Br J Ophthalmol* 2017;101:198–203.
11 Sarks SH, Arnold JJ, Killingsworth MC, *et al*. Early drusen formation in the normal and aging eye and their relation to age related maculopathy: a clinicopathological study. *Br J Ophthalmol* 1999;83:358–68.
12 Curcio CA, Medeiros NE, Millican CL. Photoreceptor loss in age-related macular degeneration. *Invest Ophthalmol Vis Sci* 1996;37:1236–49.
13 Balaratnasingam C, Messinger JD, Sloan KR, *et al*. Histologic and optical coherence tomographic correlates in drusenoid pigment epithelium detachment in age-related macular degeneration. *Ophthalmology* 2017;124:644–56.
14 Pircher M, Götzinger E, Findl O, *et al*. Human macula investigated in vivo with polarization-sensitive optical coherence tomography. *Invest Ophthalmol Vis Sci* 2006;47:5487–94.
15 Götzinger E, Pircher M, Baumann B, *et al*. Three-dimensional polarization sensitive OCT imaging and interactive display of the human retina. *Opt Express* 2009;17:4151–65.
16 Götzinger E, Pircher M, Geitzenauer W, *et al*. Retinal pigment epithelium segmentation by polarization sensitive optical coherence tomography. *Opt Express* 2008;16:16410–22.
17 Pircher M, Hitzenberger CK, Schmidt-Erfurth U. Polarization sensitive optical coherence tomography in the human eye. *Prog Retin Eye Res* 2011;30:431–51.
18 Michels S, Pircher M, Geitzenauer W, *et al*. Value of polarisation-sensitive optical coherence tomography in diseases affecting the retinal pigment epithelium. *Br J Ophthalmol* 2008;92:204–9.
19 Schlanitz FG, Baumann B, Spalek T, *et al*. Performance of automated drusen detection by polarization-sensitive optical coherence tomography. *Invest Ophthalmol Vis Sci* 2011;52:4571–9.
20 Age-Related Eye Disease Study Research Group. The age-related eye disease study (AREDS): design implications. AREDS report no. 1. *Control Clin Trials* 1999;20:573–600.
21 Baumann B, Gotzinger E, Pircher M, *et al*. Segmentation and quantification of retinal lesions in age-related macular degeneration using polarization-sensitive optical coherence tomography. *J Biomed Opt* 2010;15:061704.
22 Baumann B, Baumann SO, Konegger T, *et al*. Polarization sensitive optical coherence tomography of melanin provides intrinsic contrast based on depolarization. *Biomed Opt Express* 2012;3:1670–83.
23 Cukras C, Agrón E, Klein ML, *et al*. Natural history of drusenoid pigment epithelial detachment in age-related macular degeneration: age-related eye disease study report no. 28. *Ophthalmology* 2010;117:489–99.
24 Christenbury JG, Folgar FA, O'Connell RV, *et al*. Progression of intermediate age-related macular degeneration with proliferation and inner retinal migration of hyperreflective foci. *Ophthalmology* 2013;120:1038–45.